ADVANCED FUNCTIONAL MATERIALS
www.afm-journal.de

Normally Oriented Adhesion versus Friction Forces in Bacterial Adhesion to Polymer-Brush Functionalized Surfaces Under Fluid Flow

Jan J. T. M. Swartjes, Deepak H. Veeregowda, Henny C. van der Mei, Henk J. Busscher, and Prashant K. Sharma*

Bacterial adhesion is problematic in many diverse applications. Coatings of hydrophilic polymer chains in a brush configuration reduce bacterial adhesion by orders of magnitude, but not to zero. Here, the mechanism by which polymer-brush functionalized surfaces reduce bacterial adhesion from a flowing carrier fluid by relating bacterial adhesion with normally oriented adhesion and friction forces on polymer (PEG)-brush coatings of different softness is studied. Softer brush coatings deform more than rigid ones, which yields extensive bond-maturation and strong, normally oriented adhesion forces, accompanied by irreversible adhesion of bacteria. On rigid brushes, normally oriented adhesion forces remain small, allowing desorption and accordingly lower numbers of adhering bacteria result. Friction forces, generated by fluid flow and normally oriented adhesion forces, are required to oppose fluid shear forces and cause immobile adhesion. Summarizing, inclusion of friction forces and substratum softness provides a more complete mechanism of bacterial adhesion from flowing carrier fluids than available hitherto.

1. Introduction

Bacteria have a strong preference to adhere to and colonize surfaces by forming biofilm communities rather than remaining in a planktonic state.[1,2] Bacteria can adhere to almost any surface, which represents a major problem in both industrial and biomedical applications.[3,4] In biomedical applications, biomaterial-associated infections caused by biofilms are persistent and hard to eradicate due to their high resistance to antimicrobials.[5,6] In industrial settings, like pipelines, water treatment plants, heat exchangers, food processing equipment and on ship hulls, biofilms are associated with public health risks, lower heat transfer efficiencies and high fuel costs, respectively. Several strategies to prevent bacterial adhesion and biofilm formation have been described, either by simply changing the charge or hydrophobicity of the substratum surface or by more complex chemical modifications of the interface between bacteria and substratum surfaces.[7–10] Surface modification by means of attaching hydrophilic polymer chains in a brush configuration has been highly successful in decreasing adhesion of different bacterial strains and species by forming an osmotically driven, steric barrier to which bacteria have difficulties adhering.[11,12] Polyethylene glycol (PEG) is one of the most commonly applied polymers for creating polymer-brush coatings and these brush coatings have been shown to reduce protein adsorption and decrease bacterial adhesion by at least one order of magnitude. Although no other non-adhesive coating is able to reduce bacterial adhesion by an order of magnitude, this is still by far insufficient to prevent biofilm formation and biofilms eventually form also on polymer-brush coatings.[13,14] The mechanisms through which polymer-brushes reduce bacterial adhesion have been related to brush density and structure, resulting in strongly reduced adhesion forces between a substratum surface and a bacterium.[15–18] Attachment of polymer-brushes to a surface can be achieved by various means, like for instance adsorption mediated by hydrophobic interaction of tri-block-copolymers, or covalent grafting.[19] So far, key factor in creating a polymer-brush, effective in preventing protein adsorption and bacterial adhesion seems to be the structure of the brush.[15] However, further understanding of the influence of polymer-brush properties on bacterial adhesion is required in order to develop polymer-brush coatings with amplified reductions in bacterial adhesion.

In many industrial and bio-medical applications, bacteria approach a surface from a flowing carrier fluid attracted by non-specific, DLVO-type forces, acting in a direction normal to the substratum surface (**Figure 1**). Upon close approach of a bacterium to a surface, the bond between a substratum and an adhering bacterium may mature over time and the normally oriented adhesion force F_{adh} becomes stronger through rearrangements within the interface.[20] The influence of fluid flow on bacterial mass transport and adhesion to surfaces has been amply studied, but only tells part of the story.[21] The existence

J. J. T. M. Swartjes, Dr. D. H. Veeregowda, Prof. H. C. van der Mei, Prof. H. J. Busscher, Dr. P. K. Sharma
University of Groningen and University Medical Center Groningen
Department of Biomedical Engineering
Antonius Deusinglaan 1
9713, AV, Groningen, The Netherlands
E-mail: h.c.van.der.mei@umcg.nl

DOI: 10.1002/adfm.201400217

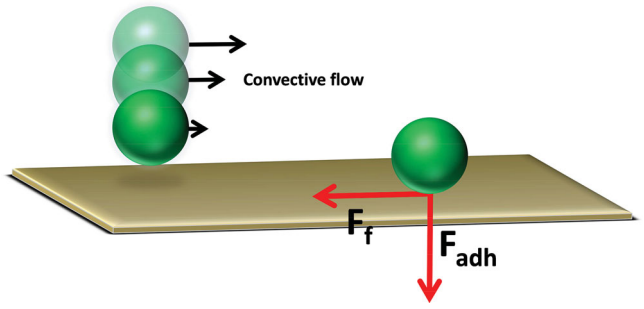

Figure 1. Forces experienced by a bacterium approaching a surface from a flowing carrier fluid. F_{adh} represents the normally oriented adhesion force between the substratum surface and a bacterium, whereas F_f represents the friction force.

of a normally oriented adhesion force in combination with convective fluid flow parallel to a surface will lead to friction forces, F_f, (Figure 1) between a bacterium and a surface that act perpendicularly to the normally oriented adhesion forces, that is, laterally to the substratum surface. The influence of normally oriented adhesion versus friction forces has never been considered in bacterial adhesion in general and the reduction of bacterial adhesion caused by polymer-brush coatings in particular.

Normally oriented adhesion forces between bacteria and surfaces can be measured with atomic force microscopy (AFM) by equipping the cantilever with a bacterial probe.[22] Similarly, using the AFM in its lateral mode, friction forces can be measured, but to our knowledge this has never been done with a bacterial probe on a material surface.[23]

The aim of this paper is to advance our understanding of the mechanisms by which polymer-brush functionalized surfaces reduce bacterial adhesion, or stated otherwise, the mechanisms by which bacteria still manage to adhere to a brush coating despite the existing, osmotically driven, steric barrier. To this end, we determine both the normally oriented adhesion and friction forces between bacteria and two distinct, self-assembling-monolayers of PEG, applied at different concentrations. Normally oriented adhesion and friction forces will be determined using AFM in its normal and lateral mode for a *Staphylococcus epidermidis* strain, while the softness of the polymer-brush coatings will be characterized using a quartz crystal microbalance with dissipation monitoring (QCM-D). All data will be related with staphylococcal adhesion to the polymer-brush coatings under convective-diffusional mass transport conditions.

2. Results

2.1. Softness of Polymer-Brush Coatings

The degree to which steric hindrance can contribute to the reduction of bacterial adhesion by polymer-brush coatings will depend in part on the softness of the brush coating. Softness can be inferred from the ratio of the change in dissipation (D) and frequency (f) of a gold-coated crystal sensor in QCM-D upon attachment of a polymer-brush to the crystal surface.[24] The softness of a polymer-brush, as expressed by the ratio ($-\Delta D/\Delta f$) varies differently with PEG-concentration for maleimide-PEG (MPEG) and PEG-thiol (TPEG; see **Figure 2**). Softness decreases with increasing concentrations of MPEG during brush formation and increases with increasing concentrations of TPEG, until a similar softness is observed for MPEG and TPEG at 80 mM. We speculate that the large differences in softness with varying concentrations of MPEG are caused by the bulky nature of its maleimide coupling group and the accompanying slower reaction rate as compared to TPEG (see Figures 2a,b), which couples directly at a much faster rate, leading to much smaller differences in softness over the range of applied concentrations.

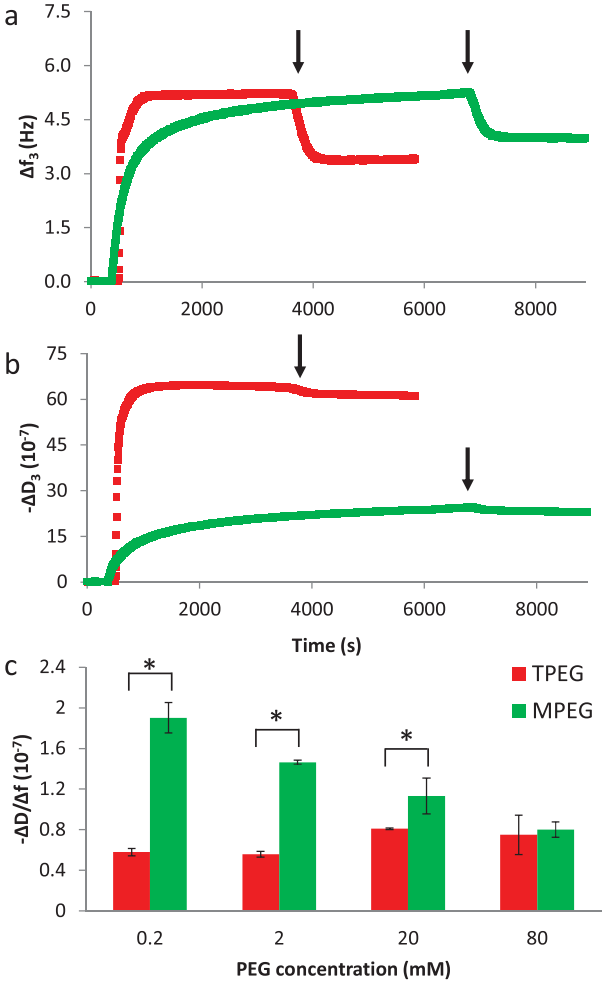

Figure 2. a) Example of the changes in frequency (Δf_3) as measured by the QCM-D for 0.2 mM TPEG and 0.2 mM MPEG. Arrows indicate start of rinsing, after frequency reached stable values. b) Example of the changes in dissipation ($-\Delta D_3$) as measured by the QCM-D for 0.2 mM TPEG and 0.2 mM MPEG. Arrows indicate start of rinsing, after dissipation reached stable values. c) Softness, expressed as the ratio ($-\Delta D/\Delta f$) obtained using QCM-D, of two different polymer-brush coatings adsorbed onto gold-coated crystal sensors from solutions with different concentrations of PEG. Smaller values of ($-\Delta D/\Delta f$) point to a more rigid brush structure. Error bars represent standard deviations over three experiments. *indicates a significant difference ($p < 0.05$) between MPEG and TPEG polymer-brushes from solutions with the same concentration.

2.2. Normally Oriented Adhesion Forces Between Bacteria and Different Polymer-Brush Coatings

Normally oriented adhesion forces between staphylococci and the different polymer-brush coatings as applied in QCM-D, were measured by approaching the coating with a staphylococcal probe until a force of 5 nN was reached and subsequently retracting the probe. The maximal force recorded during retract was taken as the normal adhesion force. In order to account for bond-maturation, both the initial adhesion force and the adhesion force after 30 s of contact were measured (see **Figure 3**a). Initial normal adhesion forces were very low (0.2 to 0.5 nN) and similar across both types of PEG coatings and all concentrations applied (see Figure 3b). However, adhesion forces after 30 s of bond-maturation decreased with increasing concentrations of MPEG and increased with increasing concentrations of TPEG until an adhesion force of 1.5 nN was reached at 80 mM. The differences in softness between TPEG and MPEG brushes were only large enough to cause significant differences in adhesion forces after 30 s bond-maturation at the two lowest concentrations applied (0.2 and 2 mM).

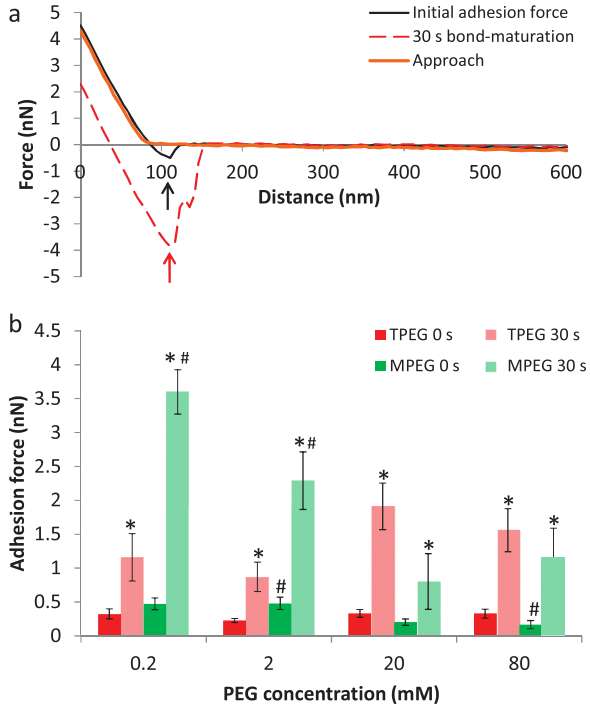

Figure 3. a) Example of a force-distance curve between *S. epidermidis* ATCC 35983 and a MPEG coating on a gold-coated wafer surface applied from a 0.2 mM solution of MPEG, taken immediately upon contact and after 30 s of bond-maturation. Arrows indicate the distances at which forces reached their maximal values upon retract. These maximal forces were taken as the normally oriented adhesion forces presented in Figure 3b. b) Normally oriented adhesion forces (F_{adh}) between *S. epidermidis* ATCC 35983 and TPEG and MPEG polymer-brush coatings prepared from PEG-solutions of different concentrations. Forces were recorded immediately upon contact between the staphylococcal probe and the coating or after 30 s of bond-maturation. Error bars represent standard errors of the mean over at least twelve force-distance curves, comprising three separately prepared coatings and bacterial probes. *indicates a significant difference ($p < 0.05$) between 0 s and 30 s adhesion forces on polymer-brush surfaces from solutions of the same concentration MPEG or TPEG. #indicates a significant difference ($p < 0.05$) between adhesion forces with the same bond-maturation time on polymer-brush surfaces of TPEG and MPEG from solutions of the same concentration.

2.3. Friction Forces Between Bacteria and Polymer-Brush Coatings

Immediately after taking force-distance curves to confirm successful attachment of bacteria to the AFM cantilever, friction forces were measured using the AFM at different applied normal forces. Friction forces were obtained upon both increasing and decreasing the normal force from 0 to 10 nN and vice versa. Coefficients of friction (COF) between the staphylococci and the polymer-brush coatings were calculated from the ratio between the measured friction force and the normal force applied. In general, friction forces were similar upon increasing or decreasing the applied normal force (**Figure 4**a). Interestingly, COFs decreased as a function of the normal force applied in a non-linear fashion, as shown in Figure 4a. Since on hard surfaces, the COF is independent of the normal force applied, this attests to the soft nature of the polymer-brush coatings. In order to deal with this effect, COFs were averaged over the values obtained for increasing and decreasing normal forces and plotted as a function of the normal forces applied on a double log-scale (Figure 4b).

Friction forces at a 1 nN applied normal force, that is, within the range of normally oriented adhesion forces between the staphylococci and the polymer-brush coatings, are presented for TPEG and MPEG polymer-brush coatings prepared from PEG-solutions of different concentrations in Figure 4c, showing a decrease in friction force with increasing MPEG concentrations in solution and little or no effect of the concentration of TPEG in solution as used for preparation of a coating.

2.4. Bacterial Adhesion Numbers and Polymer-Brush Characteristics

The numbers of staphylococci adhering to the different polymer-brush coatings were determined under convective-diffusional mass transport from a flowing carrier fluid (wall shear rate 10 s^{-1}). Adhesion experiments were continued until stable adhesion numbers over time were obtained, which usually occurred within 2 h. The numbers of staphylococci adhering after 2 h to the different polymer-brush coatings are summarized in **Figure 5** as a function of the friction force (see Figure 5a), the normally oriented adhesion force (see Figure 5b) and the softness of the polymer-brush coating (see Figure 5c). Staphylococcal adhesion numbers increased with all three brush characteristics, with the strongest correlations existing for friction force and softness.

3. Discussion

In this paper, we determined the normally oriented adhesion and friction forces between bacteria and two distinct, self-assembling-monolayers of PEG, and related these forces and

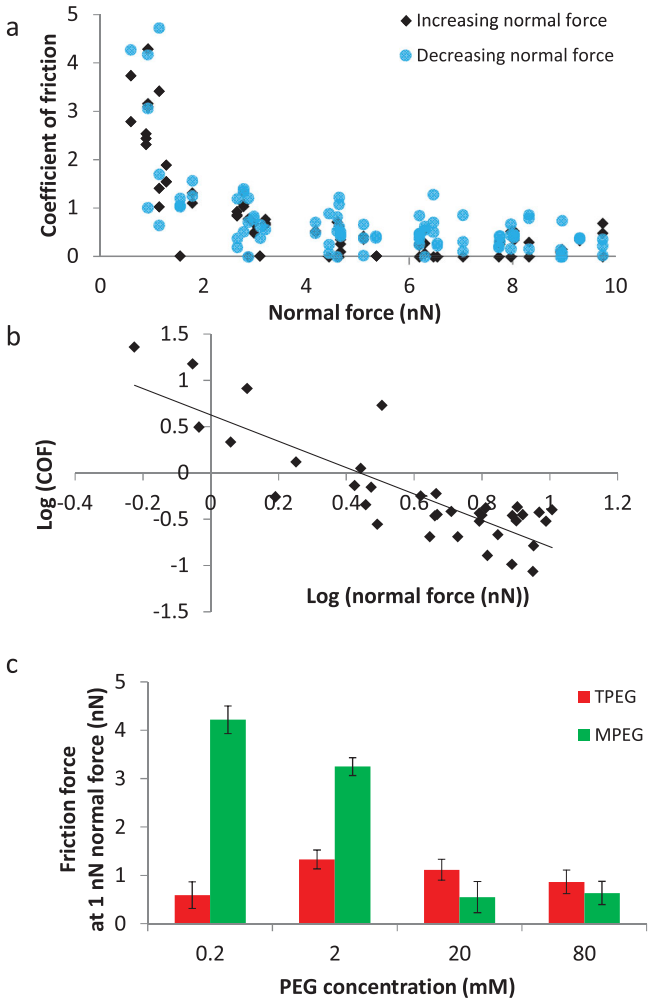

Figure 4. a) Example of the coefficient of friction (COF) as a function of normal force applied upon increasing and decreasing the normal forces for a MPEG polymer-brush coating applied from a solution of 0.2 mM MPEG. COF were calculated from the ratio between the measured friction force and the normal force applied. b) Double log-scale representation of the average COF upon increasing and decreasing the normal force (see Figure 4a), including results of a linear regression analysis (R^2 = 0.70 for the example given). c) Friction forces at a 1 nN normal force derived from linear regression analyses as shown in Figure 4b for TPEG and MPEG polymer-brush coatings prepared from PEG-solutions of different concentrations. Error bars represent standard errors of the mean over nine measurements, comprising three separately prepared coatings and bacterial probes.

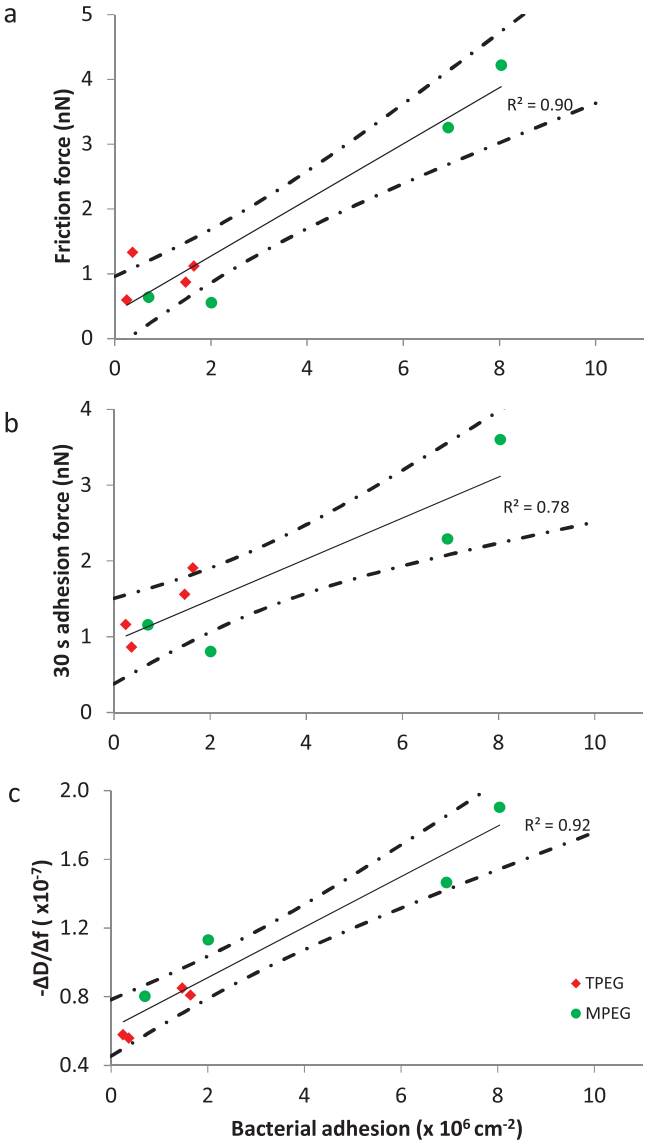

Figure 5. a) Friction forces between staphylococci and polymer-brush coatings at an applied normal force of 1 nN, as a function of bacterial adhesion numbers after 2 h of exposure of the coatings to a flowing staphylococcal suspension. b) Normally oriented adhesion forces after 30 s bond-maturation as a function of bacterial adhesion numbers after 2 h of exposure of the coatings to a flowing staphylococcal suspension. c) Softness of the polymer-brush, expressed as the ratio ($-\Delta D/\Delta f$) in QCM-D, as a function of bacterial adhesion numbers after 2 h of exposure of the coatings to a flowing staphylococcal suspension. R^2 values assuming a linear correlation are given in each graph, while the dotted lines represent the 95% confidence intervals.

the softness of the polymer-brush coatings with the number of staphylococci adhering under convective-diffusional mass transport conditions. Hitherto, studies on mechanisms of microbial adhesion have focused on normally oriented adhesion forces. However, normally oriented forces can only explain why a bacterium adheres and keeps a certain distance from a substratum surface, but cannot explain why it becomes immobilized under fluid flow, which requires forces operating laterally to a substratum surface.[25] When laterally moving bacteria encounter a surface, friction forces will arise, as demonstrated for the first time in this paper. Such friction forces can considerably slow-down bacteria in a flowing carrier fluid, to facilitate their immobile adhesion despite low, normally oriented adhesion forces.[26]

Bacteria suspended in a flowing carrier fluid adapt the velocity of the fluid, which depends on their height above the substratum surface. According to Poiseuille's law for a PPFC

$$v(y) = \frac{3}{4} \times \frac{Q_y}{b^2 w} \times \left(2 - \frac{y}{b}\right) \quad (1)$$

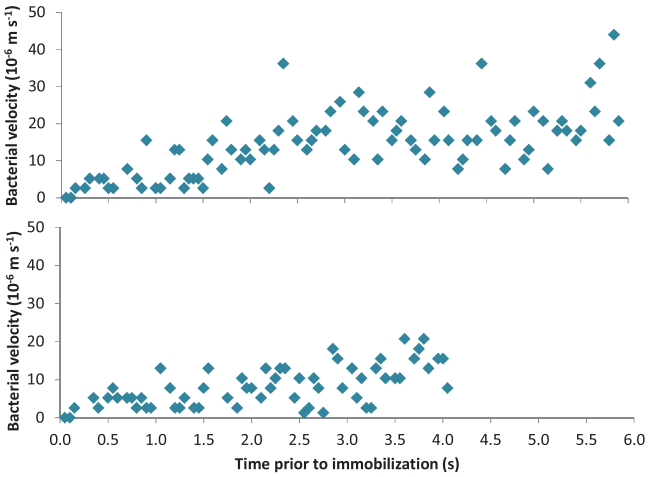

Figure 6. Examples of the velocities of two staphylococci in a flowing carrier fluid derived from image-sequence analysis as a function of the time prior to immobilization on a substratum surface modified with a 0.2 mM MPEG polymer-brush.

in which Q is the volumetric flow rate, y the perpendicular distance from the bottom plate, b the half depth of the chamber, and w its width. Close to the substratum surface, within the diffusion-boundary layer, the velocity of bacteria parallel to the surface follows from Poiseuille's law, while both its own weight and diffusion drive the suspended bacteria closer to the surface to decrease their velocity and bring them under the influence of the normally oriented adhesion forces arising from the substratum.[27] Image-sequence analysis of bacteria approaching a polymer-brush coating from a flowing carrier fluid clearly shows that once bacteria appear within the focus depth of the microscope system (up to 3 µm above the substratum surface), they have a velocity of around 20×10^{-6}–40×10^{-6} m s^{-1} (**Figure 6**). According to Equation (1), this indeed indicates that they are located in fluid flow lines approximately 3 µm above the surface, far outside the reach of the normally oriented adhesion forces arising from the substratum, but within the diffusion-boundary layer.[27] As a consequence, a diffusion-driven approach to the surface occurs resulting in contact when the velocity has decreased to around 6×10^{-6} m s^{-1} at 0.5 µm (i.e., half the staphylococcal diameter) above the surface (see also Figure 6), a phase that has been described as "mobile adhesion".[25] Mobile adhesion subsequently transforms into "immobile adhesion" as friction forces develop laterally to the substratum surface that oppose the shear force acting on the decelerating bacterium. The shear force acting on a fully immobilized bacterium follows from

$$F = \eta \times \sigma \times A_{bac} \quad (2)$$

in which η is the viscosity of the medium, σ is the shear rate and A_{bac} is the cross-sectional area of a staphylococcus. Under a fluid shear rate of 10 s^{-1}, Equation (2) allows to calculate a shear force acting on immobilized staphylococci of around 9×10^{-6} nN, which is orders of magnitude smaller than the friction forces measured in this study. Considering that shear forces arising from lateral convection are much smaller than the measured friction forces, we conclude that the friction forces are large enough to oppose the fluid shear forces and contribute to immobilization of a bacterium on the surface, needed for subsequent bond-maturation.

Once the bacterial velocity has decreased by friction arising from contact with the surface and adhesion forces have been established, the normally oriented adhesion forces increase over time and already within 30 s, a considerable maturation of the bond has occurred. The origin of this type of bond-maturation is physico-chemical in nature, as the time-scale over which it occurs in a nutrient-free suspension will not allow metabolic processes such as EPS-production, to have a major impact on the adhesion force.[20] Moreover, similar bond-maturation of normally oriented adhesion forces has been observed for inert polystyrene particles. Physico-chemical bond-maturation has been suggested to be due to removal of interfacial water, rearrangement of bacterial cell surface structures and conformational changes of cell surface macromolecules.[28] This type of bond-maturation has been associated with the residence-time dependent desorption of particles and bacteria from surfaces, based on the fact that particulate desorption disappears within 2 min, i.e., the same time-scale as over which AFM-measured adhesion forces mature to a stable value.[29]

As a new aspect of this study, we demonstrate that bond-maturation is much more extensive on softer polymer-brushes than on more rigid ones (see Figure 3B) with important consequences for bacterial adhesion. Effective polymer-brush coatings must possess a certain degree of rigidity in order to prevent their deformation under the influence of the normally oriented adhesion forces between the substratum surface and a bacterium. Therewith adhesion forces remain relatively small, allowing bacterial desorption and keeping the numbers of adhering bacteria low (**Figure 7**).[29] Soft polymer-brushes on the other hand, deform upon contact with adhering bacteria, causing more extensive bond-maturation and stronger normally oriented adhesion forces than encountered on a more rigid brush. Consequently, bacterial desorption will be low, and higher numbers of adhering bacteria will develop over time (see also Figure 7).

4. Conclusion

We showed that friction forces are involved in the adhesion and immobilization of bacteria to polymer-brush coated surfaces from a flowing carrier fluid. Friction forces are governed by an interplay of the normally oriented adhesion forces and the properties of the surface and are required to cause immobilization of adhering bacteria once they have approached the surface and established contact. On more rigid polymer-brush coatings, bacteria desorb more readily, while softer polymer-brush coatings deform upon adhesion causing a strong increase in the normally oriented adhesion force that impedes desorption. Summarizing, inclusion of both friction forces and substratum softness provides a more complete mechanism of bacterial adhesion to polymer-brush coated surfaces than can be obtained considering only normally oriented adhesion forces and will help to unveil additional options in the search for materials properties and coatings that resist bacterial adhesion. Important in this respect, is that bond-maturation after initial adhesion is avoided, which can be established with more rigid brushes.

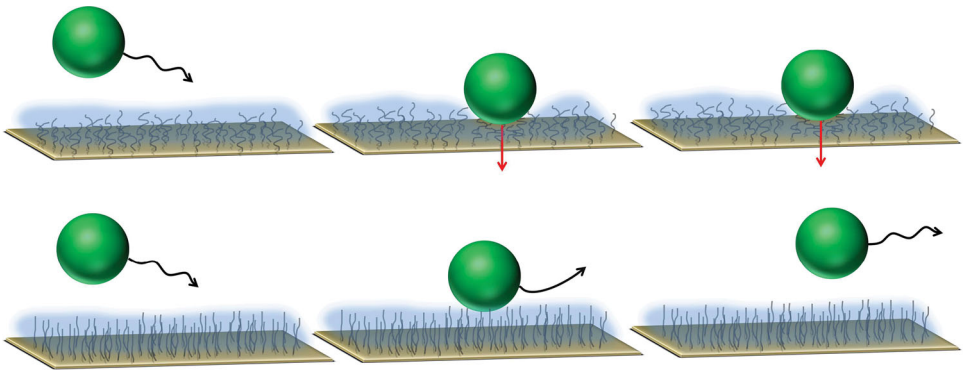

Figure 7. Schematic presentation of bacteria approaching from a flowing carrier fluid to a substratum surface and their immobilized adhesion on a soft polymer-brush (top panel) and approach to more rigid one (bottom panel), from which a bacterium readily desorbs due to the absence of deformation and extensive bond-maturation.

5. Experimental Section

O-[2-(3-mercaptopropionylamino)ethyl]-O′-methylpolyethyleneglycol 5000 (TPEG), methoxy-polyethylene glycol maleimide 5000 (MPEG), DL-dithiothreitol and octanedithiol were purchased from Sigma-Aldrich (St. Louis, USA). Ethanol (99.9%), ammonia (28–30%) and hydrogen peroxide (30%) were of analytical grade and purchased from Merck, Darmstadt, Germany.

Polymer-Brush Functionalization of Surfaces: Gold-coated silica wafers (Litcon, Gothenburg, Sweden) and gold-plated AT-cut quartz crystals (Q-sense, Gothenburg, Sweden) with a sensitivity constant of 17.7 ng cm^{-2} and a 5 MHz resonance frequency were cleaned by UV/ozone treatment followed by immersion in a 5:1:1 solution of ultrapure water (18.2 MΩ cm^{-1}, Sartorius, Göttingen, Germany), H_2O_2 and NH_3 for 10 min at 80 °C. Mono-functional PEG-thiol was attached to cleaned substrata by immersing cleaned wafers in a solution of PEG-thiol (1 mL) in ultrapure water for 30 min, or by flow of PEG-thiol solution over gold-plated quartz crystals in the QCM-D. Mono-layers of octanedithiol, required for the attachment of maleimide conjugated PEG, were formed by immersion in octanedithiol (20 mM) in ethanol and incubation in a dark, oxygen free environment for 20 h. Next, substrata were washed repeatedly with ethanol, sonicated for 2 min and washed again with ethanol before being transferred to a solution of DL-dithiothreitol (20 mM) in TRIS-HCl/EDTA (50 mM/5 mM) pH 8.0 for 2 h to re-activate the dithiol monolayer. The entire cycle of exposure to octanedithiol and DL-dithiothreitol was repeated once to obtain a homogenous monolayer.[30] Substrata were then functionalized by exposure to MPEG solution (sodium hydrogen phosphate (100 mM), EDTA (5 mM) at pH 6.5).

Softness of Polymer-Brush Coating: QCM-D (model Q-sense E4, Q-sense Gothenburg, Sweden) was used to measure the softness of the polymer-brush coatings. Polymer-brush coatings were applied by flowing a PEG solution through the QCM-D chamber at a flow rate of 2 mL h^{-1}. The QCM-D chamber is 14 mm in diameter and has a volume of approximately 40 µL. Flow with PEG solution was continued until stable values of frequency (f) and dissipation (D) where observed, which generally lasted 30 min when flowing TPEG and 120 min when MPEG was used. As soon as stable values were obtained, the crystals were washed by flow of the appropriate buffer, in order to remove unbound PEG molecules. ΔD and Δf values obtained after washing were used to evaluate the softness of the brush layer by calculating the $-\Delta D/\Delta f$ ratio, higher ratios representing softer brushes (higher dissipation shifts results from a softer brush dissipating more energy upon vibration of the crystal in an aqueous environment than in case of a more rigid brush).[24]

Normally Oriented Adhesion and Friction Forces between Staphylococci and Polymer-Brush Coatings: Staphylococci were grown overnight on blood agar plates at 37 °C for 24 h from frozen stock. Plates were kept at 4 °C and stored no longer than two weeks. Pre-cultures were prepared by inoculating single colonies from the blood agar plate into tryptone soya broth (10 mL) (TSB, OXOID, Basingstoke, England) and incubated at 37 °C for 24 h. This pre-culture was used to inoculate a main-culture of TSB (200 mL), incubated for 17 h at 37 °C. Bacteria were harvested by centrifugation for 5 min at 3000 g and washed twice using phosphate buffered saline (PBS, NaCl (150 mM), potassium phosphate (10 mM), pH 6.8). Bacterial suspension was sonicated for 3 × 10 s (Vibra Cell model 375; Sonics and Materials, USA), with 30 s breaks in between, on an ice/water bath to break up bacterial aggregates. For AFM, *S. epidermidis* ATCC 35983 was immobilized on tipless cantilevers (MikroMasch, Sofia, Bulgaria) via electrostatic interaction with poly-L-lysine (PLL; Sigma-Aldrich, USA) using a micromanipulator (manufactured by Narishige Groups, Tokyo, Japan). To this end, a droplet of PLL solution was placed on a glass slide and the far end part of the cantilever was dipped in the droplet for 1 min. After air drying (2 min), the cantilever was dipped in a droplet of a *S. epidermidis* ATCC 35983 suspension for 1 min to allow bacterial attachment to the cantilever. Bacterial probes were used for AFM immediately after preparation. Coefficients of friction and normally oriented adhesion forces towards bacteria were measured with an AFM (Nanoscope IV DimensionTM 3100) equipped with a Dimension Hybrid XYZ SPM scanner head (Veeco, NY, USA). Rectangular tipless cantilevers (length (l), width (w), and thickness (t) of 300, 35, and 1 µm, respectively) with an average stiffness of 0.05 Nm^{-1} were calibrated for their exact torsional and normal stiffness using AFM Tune IT v2.5 software.[31–33] The normal stiffness (K_n) was in the range of 0.02 to 0.08 Nm^{-1}, while the torsional stiffness (K_t) was in the range of 2 to 6 × 10^{-9} Nm rad^{-1}. The deflection sensitivity (α) of the cantilever was recorded on bare glass to calculate the applied normal force (F_n) using

$$F_n = \Delta V_n \times \alpha \times K_n \tag{3}$$

where ΔV_n is the voltage output from the AFM photodiode due to normal deflection. The torsional stiffness and estimated geometrical parameters of the bacterial probe were used to calculate the friction force (F_f) according to

$$F_f = \frac{\Delta V_L \times K_t}{2\delta\left(d + \frac{t}{2}\right)} \tag{4}$$

where t is the thickness of the cantilever, δ is the torsional detector sensitivity of the AFM and ΔV_L corresponds to the voltage output from the AFM photodiode due to lateral deflection of the bacterial probe.[32,34]

Normally Oriented Adhesion Force Measurements: In order to verify prior to and in between measurements that a bacterial probe enabled a single contact with the surface, a scanned image in AFM contact mode with a loading force of 1 to 2 nN was made at the onset of each experiment and examined for double contour lines. Double contour lines

indicate that the AFM image is not obtained from contact of a single bacterium with the surface but that multiple bacteria on the probe are in simultaneous contact with the substratum. Such probes were discarded both in the measurement of normally oriented adhesion forces as well as in friction force measurements. Force-distance curves were measured immediately upon contact and after 30 s of bond-maturation at a scan rate of 1 Hz and a trigger threshold of 5 nN. The adhesion force was calculated according to

$$F = K_n \times D \quad (5)$$

where D is the deflection of the cantilever. Force–distance curves were measured on three different spots, before and after each friction measurement to verify that the bacteria were still attached to the probe, that is, if a hard contact was observed upon approach, the probe and the measurement were discarded.

Friction Force Measurements: Lateral deflection was observed at a scanning angle of 90 degrees over a distance of 5 µm and a scanning frequency of 1 Hz. The scanning angle, distance, and frequency were kept constant throughout all friction force measurements. The bacterial probe was incrementally loaded and unloaded in steps of 0.5 nN up to a maximal normal force of 10 nN. Negative friction values, resulting from operating the AFM near its lower limits, were taken as zero.[34] COF was measured on three different spots on each substratum surface and separate bacterial probes were used for measurements on at least three separately prepared substratum surfaces. The coefficient of friction (COF) was calculated for each applied normal force rather than from the slope in the friction versus load curves, because on soft polymer brushes the COF depended in a non-linear way on the applied normal force, making it impossible to use the slope for obtaining the COF.

Staphylococcal Adhesion from a Flowing Carrier Fluid: Adhesion of *S. epidermidis* ATCC 35983 to polymer-brush coatings on the gold-coated wafers was studied using a parallel plate flow chamber, using a staphylococcal suspension with 3×10^8 bacteria mL^{-1}.[35] Prior to each experiment, the flow system was perfused with PBS to remove all air bubbles, after which the staphylococcal suspension was flown through the chamber at a constant shear rate ($10\ s^{-1}$) for 2 h. Bacterial deposition was monitored real-time using a CCD-MRXi camera (Hight Technology, Eindhoven, The Netherlands) mounted on top of a metallurgical microscope (Olympus BH-2) with a ×40 long working distance objective (depth of view 3 µm) and images were taken 2 h after flow, from which the number of adhering bacteria was determined.

Statistical Analysis: QCM-D data followed a normal distribution (Shapiro-Wilk test, $p < 0.05$) and differences between polymer-brush coatings from solutions of TPEG and MPEG of the same concentration were analyzed using Student's *t*-test. Adhesion forces were not normally distributed (Shapiro-Wilk, $p < 0.05$), and the non-parametric Kolmogorov–Smirnov test was used to compare adhesion forces. Differences were considered significant if $p < 0.05$.

Acknowledgements

This study was entirely funded by the University Medical Center Groningen, Groningen, The Netherlands. D.H.V. is also manager of Ducom Instruments Europe (Center for Innovation, L. J. Zielstraweg 2, 9713 GX, Groningen, The Netherlands), while H.J.B. is also director of a consulting company, SASA BV (GN Schutterlaan 4, 9797 PC Thesinge, The Netherlands). The authors declare no potential conflicts of interest with respect to authorship and/or publication of this article. Opinions and assertions contained herein are those of the authors and are not construed as necessarily representing views of the funding organization or their respective employers.

Received: January 21, 2014
Revised: March 4, 2014
Published online: April 7, 2014

[1] H. Flemming, J. Wingender, *Nature* **2010**, *8*, 623.
[2] L. Hall-Stoodley, J. W. Costerton, P. Stoodley, *Nat. Rev. Microbiol.* **2004**, *2*, 95.
[3] N. Høiby, O. Ciofu, H. K. Johansen, Z. Song, C. Moser, P. Ø. Jensen, S. Molin, M. Givskov, T. Tolker-Nielsen, T. Bjarnsholt, *Int. J. Oral Sci.* **2011**, *3*, 55.
[4] R. M. Donlan, *Emerg. Infect. Dis.* **2002**, *8*, 881.
[5] H. J. Busscher, H. C. van der Mei, G. Subbiahdoss, P. C. Jutte, J. J. A. M. van den Dungen, S. A. J. Zaat, M. J. Schultz, D. W. Grainger, *Sci. Transl. Med.* **2012**, *4*, 153rv10.
[6] P. S. Stewart, J. W. Costerton, *Lancet* **2001**, *358*, 135.
[7] A. K. Epstein, T. Wong, R. A. Belisle, E. M. Boggs, J. Aizenberg, *Proc. Natl. Acad. Sci. U.S.A.* **2012**, *109*, 13182.
[8] J. E. Gray, P. R. Norton, R. Alnouno, C. L. Marolda, M. A. Valvano, K. Griffiths, *Biomaterials* **2003**, *24*, 2759.
[9] J. J. T. M. Swartjes, T. Das, S. Sharifi, G. Subbiahdoss, P. K. Sharma, B. P. Krom, H. J. Busscher, H. C. van der Mei, *Adv. Funct. Mater.* **2013**, *23*, 2843.
[10] M. L. Steen, L. Hymas, E. D. Havey, N. E. Capps, D. G. Castner, E. R. Fisher, **2001**, *188*, 97.
[11] W. Senaratne, L. Andruzzi, C. K. Ober, *Biomacromolecules* **2005**, *6*, 2427.
[12] N. Ayres, *Polym. Chem.* **2010**, *1*, 769.
[13] A. L. Hook, C. Y. Chang, J. Yang, J. Luckett, A. Cockayne, S. Atkinson, Y. Mei, R. Bayston, D. J. Irvine, R. Langer, D. G. Anderson, P. Williams, M. C. Davies, M. R. Alexander, *Nat. Biotechnol.* **2012**, *30*, 868.
[14] X. Khoo, G. A. O'Toole, S. A. Nair, B. D. Snyder, D. J. Kenan, M. W. Grinstaff, *Biomaterials* **2010**, *31*, 9285.
[15] G. Gunkel, M. Weinhart, T. Becherer, R. Haag, W. T. S. Huck, *Biomacromolecules* **2011**, *12*, 4169.
[16] B. Pidhatika, J. Möller, E. M. Benetti, R. Konradi, E. Rakhmatullina, A. Mühlebach, R. Zimmermann, C. Werner, V. Vogel, M. Textor, *Biomaterials* **2010**, *31*, 9462.
[17] A. Razatos, Y. Ong, F. Boulay, D. L. Elbert, J. A. Hubbell, M. M. Sharma, G. Georgiou, *Langmuir* **2000**, *16*, 9155.
[18] Y. Wang, G. Subbiahdoss, J. Swartjes, H. C. van der Mei, H. J. Busscher, M. Libera, *Adv. Funct. Mater.* **2011**, *21*, 3916.
[19] B. Zhao, W. J. Brittain, *Prog. Polym. Sci.* **2000**, *25*, 677.
[20] H. J. Busscher, W. Norde, P. K. Sharma, H. C. van der Mei, *Curr. Opin. Colloid In.* **2010**, *15*, 510.
[21] M. G. Katsikogianni, Y. F. Missirlis, *Acta Biomater.* **2010**, *6*, 1107.
[22] L. S. Dorobantu, M. R. Gray, *Scanning* **2010**, *32*, 74.
[23] T. Filleter, R. Bennewitz, *Phys. Rev. B* **2010**, *81*, 155412.
[24] J. Malmström, H. Agheli, P. Kingshott, D. S. Sutherland, *Langmuir* **2007**, *23*, 9760.
[25] N. P. Boks, H. J. Kaper, W. Norde, H. C. van der Mei, H. J. Busscher, *J. Colloid Interface Sci.* **2009**, *331*, 60.
[26] Y. F. Dufrêne, C. J. P Boonaert, H. C. van der Mei, H. J. Busscher, P. G. Rouxhet, *Ultramicroscopy* **2001**, *86*, 113.
[27] Z. Adamczyk, T. G. van de Ven, *J. Colloid Interf. Sci.* **1981**, *80*, 340.
[28] A. Harimawan, A. Rajasekar, Y.-P. Ting, *J. Colloid Interface Sci.* **2011**, *364*, 213.
[29] V. Lo Schiavo, P. Robert, L. Limozin, P. Bongrand, *PLoS One* **2012**, *7*, e44070.
[30] A. O. Lundgren, F. Björefors, L. G. M. Olofsson, H. Elwing, *Nano Lett.* **2008**, *8*, 3989.
[31] C. P. Green, H. Lioe, J. P. Cleveland, R. Proksch, P. Mulvaney, J. E. Sader, *Rev. Sci. Instrum.* **2004**, *75*, 1988.
[32] T. Pettersson, N. Nordgren, M. W. Rutland, A. Feiler, *Rev. Sci. Instrum.* **2007**, *78*, 093702.
[33] J. E. Sader, J. W. M. Chon, P. Mulvaney, *Rev. Sci. Instrum.* **1999**, *70*, 3967.
[34] T. Pettersson, A. Naderi, R. Makuska, P. M. Claesson, *Langmuir* **2008**, *24*, 3336.
[35] H. J. Busscher, H. C. van der Mei, *Clin. Microbiol. Rev.* **2006**, *19*. 127.